Oxidation of oleic acid at the air–water interface and its potential effects on cloud critical supersaturations

Martin D. King,*[a] Adrian R. Rennie,[b] Katherine C. Thompson,[c] Fleur N. Fisher,[a] Chu Chuan Dong,[d] Robert K. Thomas,[d] Christian Pfrang[ae] and Arwel V. Hughes[f]

Received 1st April 2009, Accepted 4th June 2009
First published as an Advance Article on the web 7th July 2009
DOI: 10.1039/b906517b

The oxidation of organic films on cloud condensation nuclei has the potential to affect climate and precipitation events. In this work we present a study of the oxidation of a monolayer of deuterated oleic acid (*cis*-9-octadecenoic acid) at the air–water interface by ozone to determine if oxidation removes the organic film or replaces it with a product film. A range of different aqueous sub-phases were studied. The surface excess of deuterated material was followed by neutron reflection whilst the surface pressure was followed using a Wilhelmy plate. The neutron reflection data reveal that approximately half the organic material remains at the air–water interface following the oxidation of oleic acid by ozone, thus cleavage of the double bond by ozone creates one surface active species and one species that partitions to the bulk (or gas) phase. The most probable products, produced with a yield of $\sim(87 \pm 14)\%$, are nonanoic acid, which remains at the interface, and azelaic acid (nonanedioic acid), which dissolves into the bulk solution. We also report a surface bimolecular rate constant for the reaction between ozone and oleic acid of $(7.3 \pm 0.9) \times 10^{-11}$ cm^2 molecule s^{-1}. The rate constant and product yield are not affected by the solution sub-phase. An uptake coefficient of ozone on the oleic acid monolayer of $\sim 4 \times 10^{-6}$ is estimated from our results. A simple Köhler analysis demonstrates that the oxidation of oleic acid by ozone on an atmospheric aerosol will lower the critical supersaturation needed for cloud droplet formation. We calculate an atmospheric chemical lifetime of oleic acid of 1.3 hours, significantly longer than laboratory studies on pure oleic acid particles suggest, but more consistent with field studies reporting oleic acid present in aged atmospheric aerosol.

1. Introduction

Atmospheric aerosols are critical in determining climate and climate change of the Earth owing to their ability to scatter and absorb solar radiation, and, indirectly by acting as cloud condensation nuclei, thus controlling the formation of new clouds and precipitation.[1] It is well known that aqueous atmospheric aerosols, such as those formed from sea spray, are coated by organic surfactants[2] such as oleic acid (*cis*-9-octadecenoic acid) that may change the optical and cloud nucleation properties.[3] The fate of these films on aerosol droplets upon atmospheric oxidation of the surfactant is unknown but crucial because their oxidation strongly influences droplet growth.[4] Thick films can prevent droplets from reaching their equilibrium size by hindering water uptake,[4] whereas monolayer films of fatty acids, as considered here, lower the surface tension of the droplet and thus decrease the supersaturation ratio of water vapour required to allow droplets to grow. The topic of organic films on atmospheric particles has been reviewed by Donaldson and Vaida.[5]

Numerous previous studies on the oxidation of oleic acid by an atmospheric oxidant have been reported in the literature and laboratory experiments on oleic acid droplets reacting with ozone have been reviewed by Zahardis and Petrucci.[6] Many of the studies used either pure oleic acid droplets or a high mole fraction of oleic acid. Only a few studies focussed on the oxidation of a monolayer of oleic acid at the air–water interface.[7–9] To date no study has investigated the kinetics or observed products from reaction of ozone with a monolayer of oleic acid at the air–water interface although Wadia *et al.*[10] demonstrated that such systems could be studied using a Langmuir trough when the authors reported the gas-phase products detected following the reaction between a phospholipid containing an oleoyl tail, 1-oleoyl-2-palmitoyl-sn-glycero-3-phosphocholine, and gas-phase ozone at the air–water interface.

In this work we have used the technique of neutron reflection to determine whether the oxidation of a monolayer of oleic acid over seawater, and similar aqueous solutions, destroys the organic film or leads to the development of a new film with different physical properties. This is the first time, to

[a] *Department of Earth Sciences, Royal Holloway University of London, Egham, Surrey, UK TW20 0EX. E-mail: m.king@es.rhul.ac.uk; Fax: +44 (0)1784 471780; Tel: +44 (0)1784 414038*
[b] *Department of Physics, Uppsala University, 75121 Uppsala, Sweden*
[c] *School of Biological and Chemical Sciences, Birkbeck University of London, Malet Street, London, UK WC1E 7HX*
[d] *Physical and Theoretical Chemistry Laboratory, University of Oxford, South Park Road, Oxford, UK OX1 3QZ*
[e] *Department of Chemistry, University of Reading, Whiteknights, Reading, UK*
[f] *ISIS pulsed Neutron and Muon source, Rutherford Appleton Laboratory, Chilton, Didcot, UK OX11 0QX*

our knowledge, that neutron reflection has been used to study heterogeneous oxidation reactions occurring at the air–liquid interface.

2. Experimental

The reaction between gaseous ozone and oleic acid at the air–water interface was studied on a Langmuir trough contained in either a plastic glove bag or a 45 L aluminium gas chamber. In both cases fused quartz windows were used to allow passage of the neutrons and the laser light required for alignment. The surface excess (surface coverage) of organic material at the air–water interface was monitored by neutron reflection and the surface pressure was monitored using a Wilhelmy plate.

2.1 Neutron reflection

A full account of the use of neutron reflection to study organic molecules at the air–water interface can be found in the review by Lu *et al.*[11] but a brief description is provided here. Specular reflection of neutrons can be used to determine the composition profile normal to an interface. The reflectivity depends on the effective refractive index, n, for neutrons of the material at the interface. For any compound this can be calculated from known values of the coherent scattering lengths[12] of different nuclei as:

$$n = 1 - \frac{\lambda^2 \sum_i \frac{b_i}{V}}{2\pi} \qquad \text{(I)}$$

where $\sum_i \frac{b_i}{V}$ is the sum of scattering lengths for elements in volume V and λ is the wavelength of the neutrons. The scattering lengths of hydrogen ($b = -3.74$ fm) and deuterium ($b = 6.68$ fm) are very different and neutron reflection is an excellent means to quantify deuterated organic molecules at air–liquid interfaces.

The neutron reflection measurements were made using the CRISP and SURF reflectometers at the ISIS pulsed spallation neutron source at the Rutherford Appleton Laboratory, Chilton, UK. The incident beam with a range of wavelengths was collimated and inclined so that it fell at a grazing angle of incidence of $\theta = 1.5^\circ$ to the horizontal of the air–liquid interface. The range of neutron wavelengths, λ, provides data for the reflectivity, R, as function of momentum transfer, Q, $Q = \frac{4\pi \sin(\theta)}{\lambda}$ between about 0.06 and 0.5 Å^{-1}. All reflectivity data were normalised for the intensity of the incident beam and the absolute reflectivity obtained relative to a pure D_2O standard.

Measurements were made using various aqueous sub-phases based on a mixture of 8% (by volume) of D_2O in H_2O. The scattering length density of this D_2O–H_2O mixture is zero and thus the refractive index for neutrons is equal to that of air. In the case of this null reflecting water (NRW) the reflected signal that is observed arises only from the interfacial layer and the intensity can be easily interpreted in terms of the amount of material at the interface. For the present experiments, the data can be adequately modelled as a single uniform layer between two semi-infinite media of zero refractive index. The layer is characterised by its thickness and refractive index (or scattering length density, ρ, which is b per unit volume). A least squares fitting procedure is used to compare modelled data calculated according to Abèles optical matrix method[13] with each experimental data set measured in a time sequence. In a layer of thickness, δ, and scattering length density, ρ, the surface excess (surface coverage), Γ, of deuterium atoms with a total scattering length b_m is then given by:

$$\Gamma = \frac{\rho\delta}{b_m} \qquad \text{(II)}$$

The fitted parameters can thus be used to directly generate data for surface excess of the deuterated organic layer against time.

2.2 Generation of ozone atmosphere

Ozone was generated by exposing the flow of molecular oxygen entering the reaction chamber to UV light from a mercury pen-ray lamp. All tubing was PTFE and all connections were made of PTFE or stainless steel. The ozone concentration could be varied by part shielding the pen-ray lamp in a reproducible manner. The flow of oxygen, which was continuous throughout each experiment, was 1.0 L min^{-1} and the reaction chamber held at atmospheric pressure. The ozoniser was calibrated by measuring the absorption spectrum of the ozone from 200 to 450 nm over a 10 cm path length and applying the Beer–Lambert law.

2.3 Monitoring the surface active species

A monolayer of deuterated oleic acid ($C_{17}D_{33}COOH$, synthesised at the University of Oxford) was placed at the air–water interface of seven different null reflecting aqueous solutions. The solutions contained: (1) 33 g L^{-1} artificial sea-salt (Tropic Marin), (2) 33 g L^{-1} NaCl, (3) pure null reflecting water, (4) 35 g L^{-1} NaCl with pH adjusted to 2.4 by addition of concentrated HCl(aq), (5) 35 g L^{-1} NaCl with pH adjusted to 10.4 by addition of concentrated NaOH(aq), (6) 47.23 g L^{-1} $CaNO_3{\cdot}5H_2O$(aq), and (7) 66.62 g L^{-1} NaBr. The synthetic seawater composition was optimised for aquarium fish. It contained 70 elements with a composition approximately described by Lide[14] with the exception that the synthetic seawater contained no nitrate, phosphate or organic carbon. The synthetic seawater did not contain any surface active material. Solutions of NaCl provided a simpler proxy for aerosols with a seawater origin. The pH of the NaCl solutions was adjusted to protonate (low pH) and de-protonate (high pH) the oleic acid. The solution of $CaNO_3$ had the same ionic strength as the NaCl solution and provided a very crude proxy for aerosol containing a terrestrial component. The cation Ca^{2+} may form an insoluble soap with the monolayer. The experiments using NaBr solutions were to check for possible interference from halogen atom chemistry as ozone is over four orders of magnitude more reactive towards Br^-(aq) than it is to Cl^-(aq).[15]

The oleic acid film was spread on the surface of the bulk phase as a 1 mg mL^{-1} solution of oleic acid in chloroform using a micro-litre syringe. The reaction chamber was purged of evaporating chloroform by the flow of molecular oxygen and the film was compressed to an initial surface pressure, Π, of 10–25 mN m^{-1}. The film was then exposed to a dilute flow

of ozone in oxygen (4.2–12 $\times$ 10^{12} molecule cm^{-3}) whilst the surface coverage of deuterated material and surface pressure were recorded. During a typical measurement the surface pressure was recorded at least every second and the neutron reflectivity recorded continuously in separate intervals of 300 or 600 s. Each measurement took about 10 000 to 30 000 s.

2.4 Kinetic analysis

The aim of this work was not to investigate the kinetics of the reaction between ozone and oleic acid at the air–water interface but rather to analyse the surface coverage data so as to yield mechanistic and kinetic information. Our kinetic variable is the surface coverage of deuterium at the air–water interface, so any kinetic analysis must consider the build-up of surface active products as well as loss of oleic acid at the air–water interface. It is well known that the reaction of ozone with oleic acid will lead to initial cleavage of the double bond, but the identity of the products will depend upon the conditions (as we describe later in the discussion). A previous study of the ozone initiated oxidation of oleic acid at the air–water interface concluded that the reaction yields no surface active organic species,[7] however, our results (see later) clearly demonstrate that this is not the case and thus we considered two possible reactions in our kinetics analysis between oleic acid and ozone. Reaction (1) produces two products formed following cleavage of the double bond, one product is surface active and remains at the air–water interface, whilst the other product either partitions into the bulk aqueous or gas phase. In contrast the products of reaction (2) are not surface active. Thus, we consider a reaction that produces a surface film and one that does not. We propose that the products of reaction (1) in the presence of water are nonanoic (surface active) and nonanedioic acid (azelaic acid),

$$\begin{aligned} &CD_3(CD_2)_7CD{=}CD(CD_2)_7CO_2H + O_3 \\ &\xrightarrow{k_1} CD_3(CD_2)_7CO_2H + CO_2H(CD_2)_7CO_2H, \end{aligned} \quad (1)$$

and we do not need to identify the products of reaction (2) as they will not affect the kinetic analysis,

$$\begin{aligned} &CD_3(CD_2)_7CD{=}CD(CD_2)_7CO_2H + O_3 \\ &\xrightarrow{k_2} \text{products}. \end{aligned} \quad (2)$$

The products of reaction (1) are postulated and have not been confirmed by a separate analysis. It is conceivable that the products of reaction (1) may be different, but what we are proposing in this section is a reaction scheme consistent with producing a lower weight molecular surface active product and our kinetic results.

Cleavage of the double bond of deuterated oleic acid would initially produce two fragments, one with 15 deuteriums and the other with 18. Products with carboxylic acid groups would rapidly exchange their acidic deuterium ion for a hydrogen ion from the bulk solution thus the products would have 14 and 17 deuterium atoms, respectively.

Assuming reactions (1) and (2), the surface coverage of deuterated material at the air–water interface, Γ^t_{total}, is due to the surface coverage of deuterated oleic acid, Γ^t_{oleic}, and deuterated nonanoic acid, $\Gamma^t_{\text{nonanoic}}$, at time t,

$$\Gamma^t_{\text{total}} = 33\Gamma^t_{\text{oleic}} + 17\Gamma^t_{\text{nonanoic}} \quad \text{(III)}$$

Note that the factors of 33 and 17 represent the number of deuterium atoms in the deuterated oleic acid and the number of deuteriums in the surface active product species, which we presume is nonanoic acid. We may solve the kinetic rate equations for oleic acid oxidation assuming pseudo-first-order conditions (*i.e.* $k_A = k_1[O_3]_{\text{surf}}$ and $k_B = k_2[O_3]_{\text{surf}}$), note $[O_3]_{\text{surf}}$ is the concentration of ozone in the organic surface layer at the air–water interface:

$$\begin{aligned} \frac{d\Gamma^t_{\text{oleic}}}{dt} &= -k_A\Gamma^t_{\text{oleic}} - k_B\Gamma^t_{\text{oleic}} \\ \Rightarrow\ \Gamma^t_{\text{oleic}} &= \Gamma^{t=0}_{\text{oleic}} e^{-(k_A+k_B)t} \end{aligned} \quad \text{(IV)}$$

(where $\Gamma^{t=0}_{\text{oleic}}$ is the initial surface coverage of oleic acid and Γ^t_{oleic} is the surface coverage at time, t, later) and for the surface active product, nonanoic acid,

$$\begin{aligned} \frac{d\Gamma^t_{\text{nonanoic}}}{dt} &= +k_A\Gamma^t_{\text{oleic}} \\ \Rightarrow\ \Gamma^t_{\text{nonanoic}} &= \Gamma^{t=0}_{\text{oleic}} \frac{k_A}{k_A+k_B}(1 - e^{-(k_A+k_B)t}) \end{aligned} \quad \text{(V)}$$

Note the quantity $\frac{k_A}{k_A+k_B}$ is equal to the branching ratio for reaction (1) that is cleavage of the oleic acid chain to leave one surface active product. Substitution of (IV) and (V) into (III) gives the measured surface coverage

$$\Gamma^t_{\text{total}} = 33\Gamma^{t=0}_{\text{oleic}}\left(\left(1 - \frac{\frac{17}{33}k_A}{k_A+k_B}\right)e^{-(k_A+k_B)t} + \frac{\frac{17}{33}k_A}{k_A+k_B}\right) \quad \text{(VI)}$$

Since $\Gamma^{t=0}_{\text{total}} = 33\Gamma^{t=0}_{\text{oleic}}$ then:

$$\frac{\Gamma^t_{\text{total}}}{\Gamma^{t=0}_{\text{total}}} = \left(1 - \frac{\frac{17}{33}k_A}{k_A+k_B}\right)e^{-(k_A+k_B)t} + \frac{\frac{17}{33}k_A}{k_A+k_B} \quad \text{(VII)}$$

Thus the measured decay of surface coverage of deuterium, Γ^t_{total}, is expected to decrease exponentially with time. Note that in the above analysis we initially consider surface coverage of molecules of oleic acid and surface active product molecules but our resultant eqn (VII) depends on just the number of deuterium atoms at the surface. Fitting the temporal profiles of Γ^t_{total} to eqn (VII) allows k_A and k_B to be determined. The bimolecular rate constants for reaction of ozone with oleic acid, k_1 and k_2, in the organic monolayer can be determined from the gradient of a plot of k_A or k_B against $[O_3]_{\text{surf}}$. The concentration of ozone in the organic layer was estimated using the method of Smith *et al.*[16] *i.e.*

$$[O_3]_{\text{surf}} = [O_{3(g)}]H\delta \quad \text{(VIII)}$$

where H is the Henry's law constant for ozone between air and an organic layer and was assigned an estimated value of 480 mol m^{-3} atm^{-1} based on the work of Smith *et al.*,[16] and Morris *et al.*[17,18] The value of the layer thickness of oleic acid, δ, was taken as 2 nm based on the neutron data recorded for this work and applying eqn (II).

3. Results

Details of the experiments undertaken in the available beam time are listed in Table 1. Fig. 1 shows a plot of surface coverage *versus* time when an oleic acid monolayer was exposed to a flow of gaseous oxygen only, demonstrating that the monolayer is stable and that oxygen alone does not initiate the oxidation of oleic acid over the timescale of the experiment. Fig. 2 shows a typical plot of surface coverage *versus* time obtained when the oleic acid monolayer is exposed to gaseous ozone. The plot reveals that the amount of deuterated material at the air–water interface approximately halves following the reaction of oleic acid with ozone. The approximate halving of the amount of deuterated material at the air–water interface was repeated in all twenty-three separate experiments, as shown in Table 1, the fourth column of which displays the ratio of the initial to final surface coverage of deuterium atoms, $\frac{\Gamma_{\text{final}}}{\Gamma_{\text{initial}}}$. The average value of $\frac{\Gamma_{\text{final}}}{\Gamma_{\text{initial}}}$ is 0.51 ± 0.06. The error is propagated from the statistical fit uncertainties in calculating the surface coverage from the neutron reflectivity data. Table 2 shows the mean value of $\frac{\Gamma_{\text{final}}}{\Gamma_{\text{initial}}}$ for the seven different sub-phases and demonstrates that, at least for the range of sub-phases considered here, the nature of the sub-phase does not change the value of $\frac{\Gamma_{\text{final}}}{\Gamma_{\text{initial}}}$. Thus, regardless of the sub-phase approximately half of the oleic acid molecule is left at the air–liquid interface following oxidation by gas-phase ozone. The halving of the deuterated material at the oxygen–water interface is consistent with cleavage of the double bond of oleic acid by ozone to form two products, one of which remains at the air–water interface whilst the other is either incorporated into the bulk (solubilised) or released into the gas phase.

It is worth noting that Fig. 2 also demonstrates that the decay of the surface coverage of deuterium atoms at the air–water interface with time, as measured by neutron reflection, is reproduced by the change in surface pressure of the material at the air–water interface as measured by the Wilhelmy plate. Thus the kinetics of decay of oleic acid at the air–water interface could be studied by the Wilhelmy plate method, an important result for future kinetic studies.

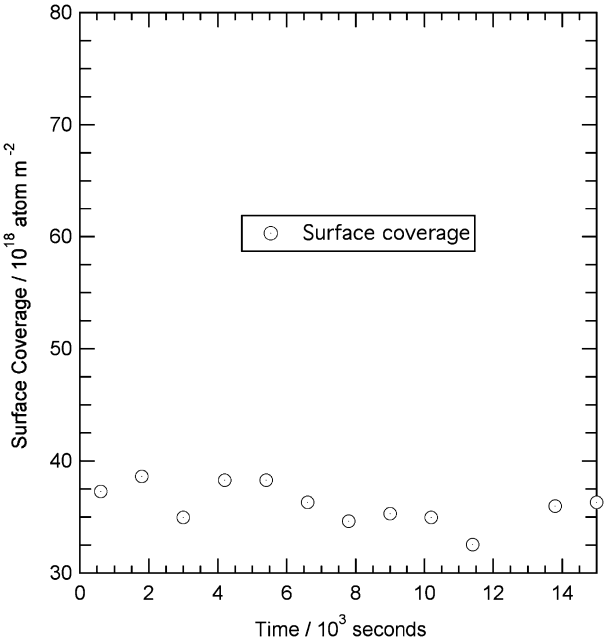

Fig. 1 Plot of the surface coverage of deuterium, Γ, (left axis, open circles) *versus* time measured when a film of deuterated oleic acid on synthetic seawater was exposed to gas-phase oxygen, *i.e.* blank run.

The values obtained for k_A and k_B from fitting eqn (VII) to the neutron reflection data are given in Table 1. The last column of Table 1 gives the branching ratio, $\frac{k_A}{k_A+k_B}$, for the

Table 1 Details of the experiments undertaken and the results obtained by fitting eqn (VII) to the experimental data (note, an error of ±0 indicates that the value was held constant during the fitting, rather than allowed to vary)

				Results from fitting eqn (VII)			
Sub-phase	pH	$[O_{3(g)}]/10^{12}$ molecule cm^{-3}	$\frac{\Gamma_{\text{final}}}{\Gamma_{\text{initial}}}$	$\Gamma^{t=0}_{\text{oleic}}/10^{18}$ molecule m^{-2}	$k_A/10^{-4}$ s^{-1}	$k_B/10^{-4}$ s^{-1}	$\frac{k_A}{k_A+k_B}$
Water	—	4.2	0.54	0.896 ± 0.125	2.76 ± 1.48	1.04 ± 0.572	0.73 ± 0.49
Artificial seawater	—	4.2	0.53	1.09 ± 0.0215	2.04 ± 0.249	0.336 ± 0.0519	0.86 ± 0.14
Artificial seawater	—	4.2	0.47	2.50 ± 0.0331	2.89 ± 0.195	0.758 ± 0.062	0.79 ± 0.07
Artificial seawater	—	4.2	0.47	1.09 ± 0.0535	3.06 ± 1.21	0.770 ± 0.274	0.80 ± 0.41
$NaCl_{(aq)}$	6.2	16.0	0.46 ± 0.04	1.80 ± 0.0854	32.1 ± 5.99	3.21 ± 1.94	0.91 ± 0.26
$NaCl_{(aq)}$	6.2	16.0	0.53 ± 0.06	1.9 ± 0	19.8 ± 9.52	0.743 ± 2.00	0.96 ± 0.67
$NaCl_{(aq)}$	6.2	16.0	0.51 ± 0.07	1.53 ± 0.124	33.0 ± 4.60	1.04 ± 2.75	0.97 ± 0.21
$NaCl_{(aq)}$	6.2	8.5	0.48 ± 0.10	1.74 ± 0.0591	13.7 ± 1.97	1.86 ± 0.55	0.88 ± 0.19
$NaCl_{(aq)}$	6.2	4.2	0.39 ± 0.16	1.79 ± 0.0802	1.89 ± 1.22	2.66 ± 0.245	0.42 ± 0.70
$NaCl_{(aq)}$	6.2	12.8	0.56 ± 0.14	2.0 ± 0	9.80 ± 10.4	0.500 ± 2.80	0.95 ± 1.49
$NaCl_{(aq)}$	6.2	16.0	0.60 ± 0.08	2.23 ± 0.108	22.1 ± 5.36	0.680 ± 1.15	0.97 ± 0.34
Water	6.2	16.0	0.46 ± 0.08	2.02 ± 0.308	23.0 ± 4.82	4.65 ± 4.68	0.83 ± 0.32
Water	6.2	4.2	0.56 ± 0.12	2.06 ± 0.124	8.22 ± 2.20	8×10^{-18} ± 0.486	1.00 ± 0.38
$NaCl_{(aq)}$	2.4	4.2	0.52 ± 0.28	1.92 ± 0.182	4.74 ± 2.61	0.908 ± 0.568	0.84 ± 0.73
$NaCl_{(aq)}$	2.4	8.5	0.59 ± 0.22	2.00 ± 0.194	15.0 ± 8.82	0.477 ± 1.93	0.97 ± 0.83
$NaCl_{(aq)}$	10.1	4.2	0.54 ± 0.34	1.59 ± 0.106	9.09 ± 2.73	0.399 ± 0.751	0.96 ± 0.42
$NaCl_{(aq)}$	10.1	8.5	0.49 ± 0.20	2.00 ± 0.407	15.4 ± 4.13	3.92 ± 4.22	0.80 ± 0.41
$NaCl_{(aq)}$	10.1	4.2	0.51 ± 0.26	1.80 ± 0.104	5.38 ± 2.02	1.485 ± 0.438	0.78 ± 0.48
$CaNO_{3(aq)}$	7.2	4.2	0.45 ± 0.21	2.06 ± 0.227	6.43 ± 2.12	2.09 ± 0.977	0.75 ± 0.43
$CaNO_{3(aq)}$	7.2	8.5	0.47 ± 0.21	1.90 ± 0.261	11.4 ± 5.41	2.98 ± 2.24	0.79 ± 0.62
$CaNO_{3(aq)}$	7.2	8.5	0.47 ± 0.24	1.80 ± 0.0707	18.7 ± 3.24	1.08 ± 0.879	0.95 ± 0.24
$NaBr_{(aq)}$	7.2	8.5	0.56 ± 0.25	1.92 ± 0.0633	20.4 ± 2.56	1.00×10^{-6} ± 0.68	1.00 ± 0.18
$NaBr_{(aq)}$	7.2	4.2	0.54 ± 0.25	1.98 ± 0.0618	11.7 ± 1.55	0.113 ± 0.383	0.99 ± 0.19

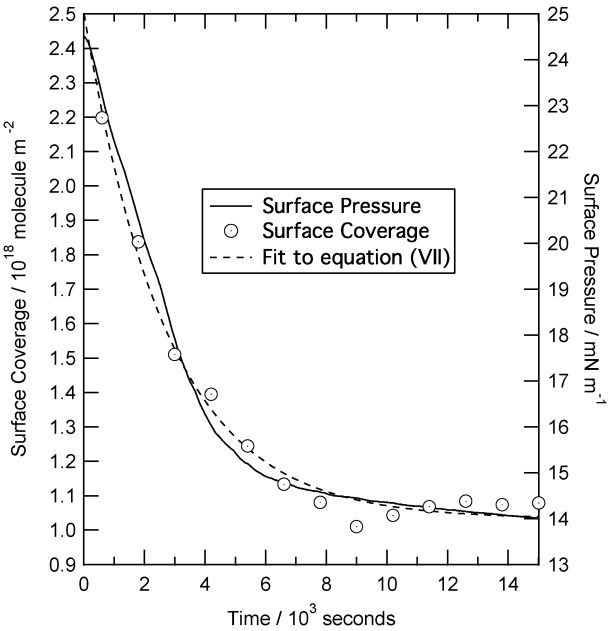

Fig. 2 Plot of surface coverage of deuterium (left axis, open circles) and surface pressure (right axis, solid line) *versus* time measured when a film of deuterated oleic acid on synthetic seawater was exposed to gas-phase ozone.

channel leading to the formation of one surface active species and one bulk phase species from the reaction of ozone with oleic acid at the air–water interface. The average branching ratio for all twenty-three experiments is 0.86 ± 0.05 and the branching ratios for all experiments agree within error, again demonstrating that the sub-phase does not affect the products of the reaction. It should be noted that the value of $\frac{\Gamma_{final}}{\Gamma_{initial}}$ obtained, 0.51 ± 0.06, implies a branching ratio for reaction (1) of 1.0 ± 0.1 and is thus consistent, within error (a standard deviation), with the value obtained from the kinetic analysis, 0.86 ± 0.05. The kinetic analysis has the advantage, however, of considering all data points collected, rather than just those measured at the beginning and end of the reaction.

Table 2 The variation of $\frac{\Gamma_{final}}{\Gamma_{initial}}$ and $\frac{k_A}{k_A+k_B}$ with the composition of the sub-phase

Sub-phase	pH	$\frac{\Gamma_{final}}{\Gamma_{initial}}$	$\frac{k_A}{k_A+k_B}$
$NaCl_{(aq)}$	6.2	0.50 ± 0.04	0.91 ± 0.11
$NaCl_{(aq)}$	2.4	0.55 ± 0.05	0.90 ± 0.55
$NaCl_{(aq)}$	10.1	0.51 ± 0.07	0.85 ± 0.25
Water	6.2	0.52 ± 0.05	0.87 ± 0.22
$CaNO_{3(aq)}$	7.0	0.47 ± 0.05	0.89 ± 0.20
$NaBr_{(aq)}$	7.2	0.55 ± 0.05	1.00 ± 0.13
Artificial seawater	7.2	0.48	0.80 ± 0.13

To calculate the 'surface' bimolecular reaction rate coefficient for the reaction between ozone contained in the organic layer and oleic acid to yield a surface active species and a non-surface active species (reaction (1)) and purely non-surface active products (reaction (2)), the first-order rate constants obtained from fitting eqn (VII) to the temporal neutron reflection data are plotted *versus* the surface concentration of ozone in the organic film, $[O_3]_{surf}$, as shown

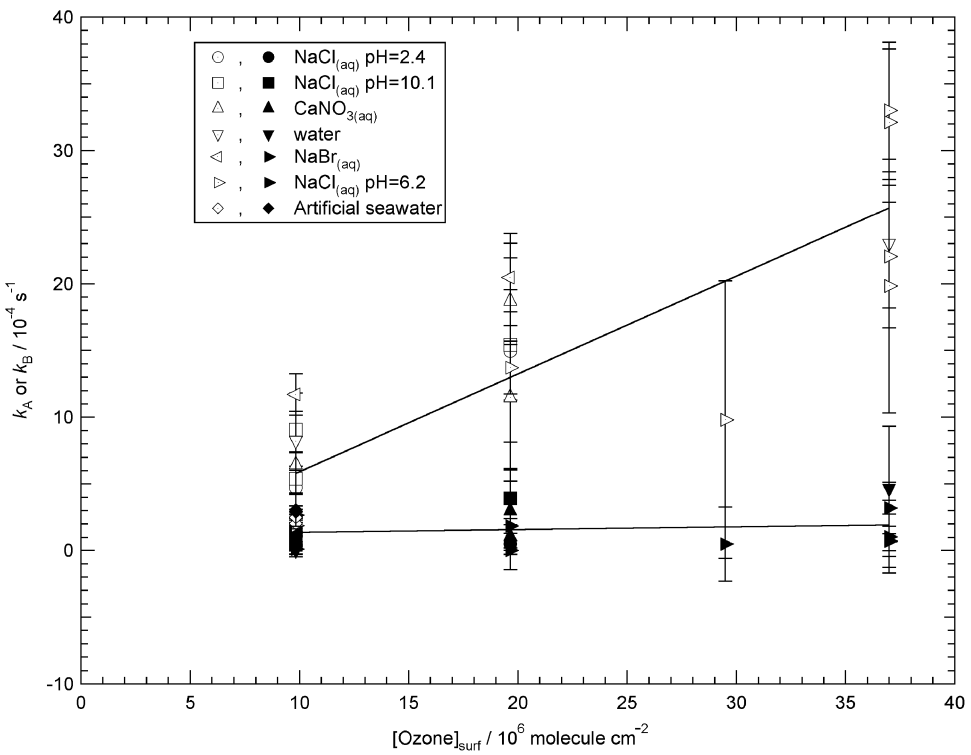

Fig. 3 A plot of measured first-order rate constants for reaction between a monolayer of oleic acid with ozone and the ozone concentration in the organic layer. The open symbols represent values for k_A (reaction between ozone and oleic acid to form nonanoic acid) and the filled symbols values for k_B (reaction between ozone and oleic acid to form a non-surface active product). The error bars are statistical and represent the uncertainty in fitting data such as displayed in Fig. 2. Different symbol shapes correspond to different sub-phase compositions. The lines represent the results of linear regression.

in Fig. 3. From Fig. 3 values of $k_1 = (7.3 \pm 0.93) \times 10^{-11}$ and $k_2 = (2.1 \pm 2.7) \times 10^{-12}$ cm^2 molecule^{-1} s^{-1} are obtained.

4. Discussion

The discussion will focus on the comparison of our measurements with other studies of the oxidation of oleic acid with ozone, the extraction of kinetic and uptake data from our measurements and the atmospheric implications of our findings.

4.1 Comparison to previous studies of the oleic acid–ozone reaction at the air–water interface

There have been several studies of the oxidation of oleic acid at the air–water interface.[7–9] The work presented here, demonstrating that an oxidation product remains at the air–water interface after oleic acid is oxidised by gas-phase ozone, does not agree with the conclusions of Voss *et al.*[7] Voss *et al.*[7] oxidised oleic acid at both the air–water and air–saltwater interface with ozone and monitored the loss of oleic acid at the interface by sum frequency generation spectroscopy. Voss *et al.*[7] stated that any oxidation products of the oleic acid (with an acyl chain) dissolved in the bulk or volatilised rather than remain at the air–water interface, in contrast to what we report in this work. In separate experiments Voss *et al.*[7] noted that the there was ''no spectroscopic evidence of nonanoic acid or azelaic acid (nonanedioic acid) when five monolayer's equivalent were spread at the air–water interface''. However, Caetano *et al.*[19] demonstrated that ''nonanoic acid quickly migrates to the aqueous–air interface independently of the preparation procedure'' in their work following the photolysis of DOPC vesicles, and work by Gilman *et al.*[20] reports a nonanoic acid isotherm by adding less than the 5 equivalent monolayers of material to the air–water interface. Thus we suggest that the system used by Voss *et al.*[7] was not sensitive to the presence of relatively short chain species such as nonanoic acid at the air–water interface when the surface pressure is low. This conclusion is supported by the fact that sum frequency generation spectroscopy is sensitive to both the number density of molecules at the interface and the orientation of the molecules, as has been demonstrated previously by Voss and co-workers.[21]

González-Labrada *et al.*[8,9] studied the oxidation of a monolayer of oleic acid at the air–water interface using a pendant drop apparatus. González-Labrada *et al.* demonstrated that the kinetic decay of oleic acid and uptake coefficient of ozone on the film can be calculated by following the changes in the surface pressure of the film.[9] The authors fitted a polynomial to describe the relationship between the surface coverage of oleic acid and surface pressure based on the quantity of oleic acid added to the film, the droplet surface area and an isotherm for oleic acid. However in our work presented here we directly measure the surface coverage of deuterated material and note it has the same temporal decay profile as the surface pressure, thus validating their method.

There are several studies of self-assembled monolayers of oleic acid on silica reacting with ozone and other gases. We have not compared our results with these studies as the water sub-phase is essential for the reaction mechanisms considered here.

4.2 Products of the reaction between ozone and oleic acid at the air–water interface

Many studies report products from the reaction between oleic acid and ozone as: azelaic acid (nonanedioic acid), nonanoic acid, nonanal and 9-oxononanoic acid.[4,16,17,22–27] Several studies have also reported polymerisation and oligomer formation during the reaction between oleic acid and ozone to make higher molecular weight products than the starting material.[27–29] The majority of the studies, including all of those that reported higher molecular weight products, are for products formed in the reaction of ozone either with pure oleic acid particles or for oleic acid particles mixed with other organic species.

For the ozonolysis of pure oleic acid (in the absence of water) it is the secondary reactions of the stabilised Criegee intermediate with carbonyl species present that lead to the product distributions noted by others.[16,17,22–25,27] These studies are all undertaken in either pure or extremely concentrated oleic acid particles (or thick films) where the reaction between the stabilised Criegee intermediate and another carbonyl species is likely to be dominant. Zahardis and Petrucci review this complex chemistry.[6] McNeill *et al.* present a product study of the reaction of thin films on aqueous solutions and note that the major products are nonanoic acid, azelaic acid and 9-oxononanoic acid.[30]

The quoted aqueous solubility of azelaic acid (2.4 g L^{-1})[31] is an order of magnitude greater than that of nonanoic acid (0.28 g L^{-1}),[20] thus the azelaic acid formed dissolves into the bulk leaving nonanoic acid at the surface, decreasing the surface coverage of deuterated material by a factor of 15/33 = 0.52, and decreasing the surface pressure. This conclusion is entirely consistent with the results of our neutron reflection studies, however, we wish to stress that whilst we have clearly demonstrated that an organic species is left at the air–water interface following the oxidation of an oleic acid monolayer by ozone, and that the data are consistent with this organic species being nonanoic acid, we have not, as yet, undertaken experiments to directly identify the product species at the interface. The solubility of 9-oxononoaic acid is expected to lie between azelaic and nonanoic acid. If 9-oxononanoic acid were surface active and a major product in our experiments then the surface coverage of deuterated material could be expected to decrease by 17/33 = 0.45 during reaction, which is not consistent with our results.

4.3 Kinetic analysis

The kinetics analysis method we use in this paper is only valid if the concentration of ozone in the organic layer is in equilibrium with the gas-phase concentration of ozone. It is instructive to compare the characteristic times, τ, for (1) diffusion of ozone to the organic surface from the bulk gas, $\tau_{diffusion}$, and (2) the interfacial accommodation of the ozone, $\tau_{interfacial}$, with the characteristic time for reaction of oleic acid with ozone, τ_{react}. Using the characteristic time calculations detailed in ref. 32, a characteristic distance of 20 Å (thickness of oleic acid film), diffusion constants of 1.8×10^{-5} m^2 s^{-1} and 1.0×10^{-9} m^2 s^{-1} for ozone in the gas-phase and organic liquid and a first-order reaction rate

Table 3 Characteristic time for ozone diffusion, interfacial accommodation and reaction with oleic acid. Equations from Seinfeld and Pandis.[32] A characteristic distance, d, of 20 Å (thickness of oleic acid film), diffusion constants of $D_g = 1.8 \times 10^{-5}$ m^2 s^{-1} and $D_l = 1.0 \times 10^{-9}$ m^2 s^{-1} for ozone in the gas-phase and organic liquid and a first-order reaction rate constant of $k = 10^{-3}$ s^{-1} were used

Process	Equation	Characteristic time, τ/s
Gas-phase diffusion	$\tau_{\text{diffusion}} = \frac{d^2}{4D_g}$	$\sim 6\times10^{-14}$
Interfacial equilibrium	$\tau_{\text{interfacial}} = \frac{d^2}{\pi^2 D_l}$	$\sim 3\times10^{-10}$
Reaction	$\tau_{\text{reaction}} = \frac{1}{k_{\text{surf}}\Gamma_{\text{oleic}}}$	10^3

constant of 10^{-4} s^{-1} we show in Table 3 that the characteristic time for reaction is much larger than the other processes and thus our analysis method is sound.[32]

Our results lead to a value of $(7.3 \pm 0.9) \times 10^{-11}$ cm^2 molecule^{-1} s^{-1} for the surface bimolecular rate coefficient for reaction (1). González-Labrada *et al.*[9] have also measured the kinetics of the reaction between a monolayer of oleic acid and ozone and report a second-order surface rate constant of 4.9×10^{-11} cm^2 molecule^{-1} s^{-1}. The agreement with our own value is excellent considering the entirely different experimental methods and detection systems employed.

It was not the aim of this work to undertake a detailed kinetic analysis, thus the reaction between oleic acid and ozone was not studied over a large range of ozone concentrations. No curvature in the plot of k_A *versus* $[O_3]_{surf}$ is apparent and thus Langmuir–Hinshelwood kinetics cannot be confirmed for this system as they have for other monolayer systems *e.g.* ref. 29, 30 and 33. However the work by González-Labrada *et al.*[9] and Hearn *et al.*[23] suggest the reaction of ozone with oleic acid is solely a surface reaction. McNeill *et al.*[30] used a Langmuir–Hinshelwood equation to explain the non-linear variation with ozone concentration of the first-order rate constant for the reaction of methyl oleate with ozone.

4.4 Uptake coefficients

Using the analysis of Hearn *et al.*,[23] which was also used by González-Labrada *et al.*,[9] we can estimate an uptake coefficient, γ, for ozone on a droplet containing a monolayer of oleic acid using

$$\gamma = \frac{4HRT}{\bar{c}}\delta k^{\text{surf}}\Gamma_{\text{oleic}} \qquad \text{(IX)}$$

where H is the Henry's law constant (480 mol m^{-3} atm^{-1}),[34] R is the gas constant (8.204×10^{-5} atm m^3 mol^{-1} K^{-1}), T is the temperature (293 K), $\bar{c}$ is the average molecular speed of the gas (360 m s^{-1}), δ is the thickness of the film of the surface layer (into which O_3 diffuses, *i.e.* 20×10^{-10} m), k^{surf} is the surface reaction rate constant between ozone and oleic acid ($k^{\text{surf}} = 7.3 \times 10^{-11}$ cm^2 molecule^{-1} s^{-1}) and Γ_{oleic} is the surface concentration (or surface coverage 2×10^{18} molecule m^{-2}) of oleic acid. The neutron reflection technique allowed us to measure values of δ for an oleic acid monolayer and values were ~19–20 Å. These values result in $\gamma \sim 4 \times 10^{-6}$ that is comparable to the value obtained by González-Labrada *et al.*[9] of $\gamma = (2.6 \pm 0.1) \times 10^{-6}$ (it is not clear from ref. 9 which values were used in eqn (IX)). Uptake coefficients reviewed by Zhardis and Petrucci[6] for ozone uptake on particles containing pure oleic acid or oleic acid mixed with another organic species suggest a value of $\sim 8 \times 10^{-4}$, significantly different from our result and that of González-Labrada *et al.*[9] No reasons are offered at present for these large differences but it should be noted that a monolayer of oleic acid at the air–water interface is a very different environment to the surface of a bulk organic liquid as has been shown previously by McNeill *et al.* and Moise and Rudich.[30,35] Moise and Rudich demonstrated that the uptake coefficient for a reaction between a monolayer of a terminal alkene with ozone was approximately an order of magnitude less than an uptake coefficient measured for the same terminal alkene as a bulk liquid reacting with ozone.[35] The authors showed that the diffuso-reactive length for the reaction of ozone with the bulk terminal alkene was larger than the monolayer. Thus in the case of reaction between ozone and the bulk terminal alkene there must be a mechanism for loss of ozone owing to solvation and reaction with double bonds deeper in the liquid. McNeill *et al.* demonstrated the same effect for the reaction of ozone with presumed sodium oleate monolayers on aqueous aerosols (containing NaCl and Na_2SO_4).[30]

4.5 Atmospheric implications: chemical lifetime

The atmospheric lifetime of oleic acid in a particle owing to reaction with ozone can be calculated from the reciprocal of the first-order rate constant for reaction between gas-phase ozone and oleic acid. Thus for a typical atmospheric concentration of ozone of 50 ppb, the first-order loss of oleic acid corresponds to an atmospheric lifetime of ~1.3 hours, significantly longer than the values quoted by other workers (typically 10 minutes) *e.g.* ref. 24, 25 and 36. Oleic acid has been found in aged aerosols (2–3 days)[17,37] and our longer lifetime is thus more likely than the previous values of ~10 minutes. Other authors have reconciled the occurrence of oleic acid in aged aerosols with its fairly short lifetime by suggesting phase and composition of the aerosol may retard oleic acid oxidation.[17,24,36] McNeill *et al.* discuss the issue of atmospheric aerosol monolayers being composed of a mixture of surfactants and they speculate how this may alter the uptake and kinetics of oxidation.[30]

4.6 Atmospheric implications: investigation of Köhler behaviour

The oxidation of a monolayer of oleic acid on a droplet of saltwater in the atmosphere will affect the hygroscopic behaviour of the droplet. The oxidation will (a) increase the surface tension of the droplet by replacing an oleic acid monolayer with a nonanoic monolayer at the air–water interface, (b) increase the ionic strength of the droplet owing to the azelaic acid dissolving into the bulk of the droplet and (c) increase the amount of insoluble material in the droplet for low water contents *i.e.* the concentration of the azelaic acid will exceed the solubility in the available water. We choose two examples here to describe the hygroscopic behaviour of this system and note a full and thorough analysis with a cloud microphysics model would be preferable.

We assume a water droplet of radius 0.1 μm is generated from sea spray with an aqueous composition of $[NaCl_{(aq)}] = 0.56$ mol dm^{-3} (to represent sea water) and either (a) a single

monolayer of oleic acid ($\Gamma = 4 \times 10^{18}$ molecule cm^{-2}) or (b) the equivalent of three monolayers of oleic acid. At surface pressures greater than $\sim$30 mN m^{-1} the oleic acid will form 'lenses' of pure oleic acid at the air–water interface which are in equilibrium with a monolayer of oleic acid.[38] We will compare the hygroscopic curve of supersaturation *versus* droplet radius for similar droplets of (i) a simple aqueous NaCl droplet with no oleic acid present, (ii) an aqueous droplet of $NaCl_{(aq)}$ with oleic acid and (iii) an aqueous droplet of NaCl with a nonanoic monolayer and azelaic acid in the bulk solution. The concentration of NaCl(aq) for all three particles will be the same and the amount of azelaic and nonanoic acid will equal the initial amount of oleic acid. We will use the following form of the Köhler equation based on the work of Shulman *et al.*:[39]

$$\frac{P}{P_0} \cong 1 + \underbrace{\frac{2\gamma M_w}{kT\rho r}}_{\text{Kelvin effect}} + \underbrace{\frac{3M_w\Phi}{4\pi\rho}\left(\frac{\chi_{organic}\nu_{organic}m_{organic}}{M_{organic}} + \frac{\nu_{salt}m_{salt}}{M_{salt}}\right)}_{\text{Raoult effect}} \times \underbrace{\left(\frac{1}{r^3} - \frac{1}{r_{insoluble}^3}\right)}_{\text{insoluble effect}} \quad (X)$$

where P is the vapour pressure of water over a droplet of radius r, P_0 is the vapour pressure over a flat surface of solution, γ is the surface tension of the solution, M_w is the molecular weight of water, R is the gas constant, T is the temperature (296 K), ρ is the solution density ($\sim$1 kg dm^{-3}), Φ is the osmotic coefficient of the solution ($\sim$1), χ is the degree of dissociation of any sparingly soluble species (*i.e.* azelaic acid; note that nonanoic and oleic acids are considered insoluble), $\nu_{organic}$ is the number of ions that the organic acid (azelaic) will dissociate into ($\nu_{organic} = 2$), $m_{organic}$ is the mass of organic material in solution, $M_{organic}$ is the molecular mass of the organic material, ν_{salt}, m_{salt} and M_{salt} are the number of ions that the salt (NaCl) dissociates into (2), the mass of salt in the droplet and the molecular mass of the salt, respectively, $r_{insoluble}$ is the radius of the volume of material that has not dissolved into the droplet. The variation of surface tension with particle surface area for the oleic and nonanoic acid films is taken from the isotherm measurements of Gilman[20] and Labourdenne.[40]

The results of these calculations are plotted in Fig. 4, for particles containing 1 and 3 monolayers of oleic acid. Two results are immediately obvious: (1) the oxidation of oleic acid lowers the critical supersaturation required for droplet (and thus cloud) formation and thus promotes cloud formation; (2) the surface tension effect of a single monolayer of oleic acid during particle formation does not have any effect on the critical supersaturation point of a droplet.

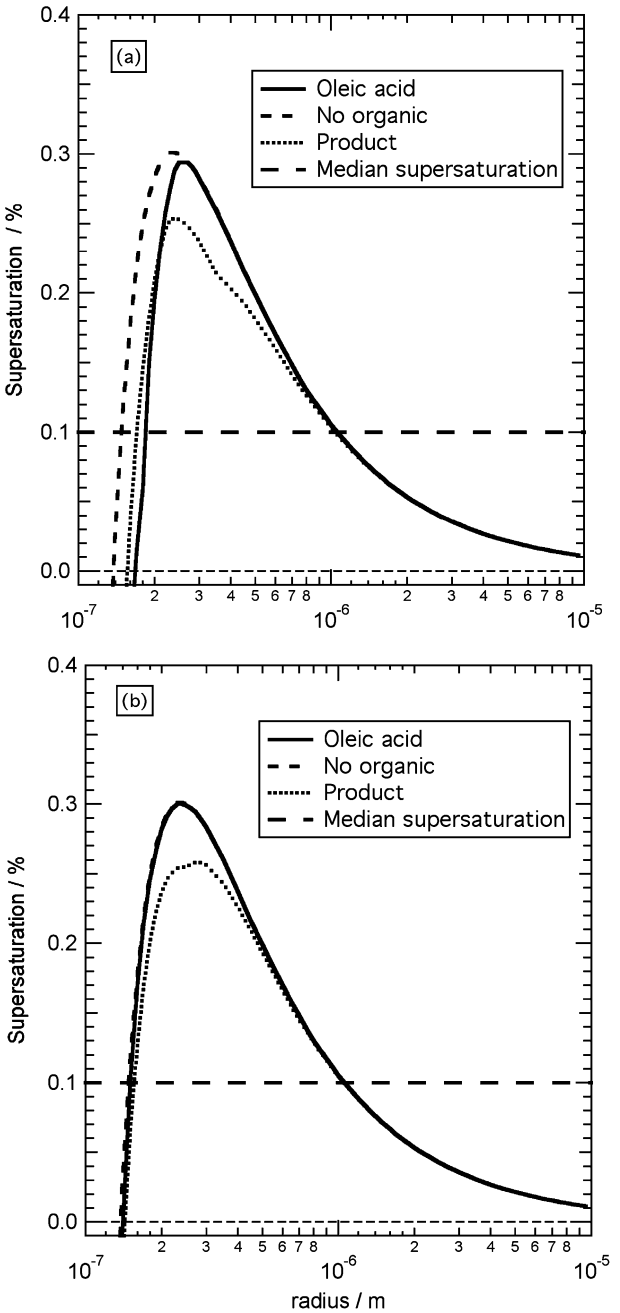

Fig. 4 Representative Köhler curves for three particles containing just $NaCl_{(aq)}$ (dashed line), $NaCl_{(aq)}$ with oleic acid (solid line) and $NaCl_{(aq)}$ with azelaic and nonanoic acids (dotted line). The three droplets show the effect on the hygroscopicity of oleic acid and the oxidation products of ozone and oleic acid. Calculations are based on an initial particle with a 0.1 μm radius containing 0.56 mol dm^3 [NaCl] and either one monolayer of oleic acid (b) or the equivalent of three monolayers of oleic acid (a). The median cloud supersaturation is also plotted. The complete oxidation of oleic acid will move the particle from the solid line to the dotted line, *i.e.* lowering the critical supersaturation point.

5. Conclusions

We can reach three clear conclusions from this work:

(a) The oxidation of an oleic acid monolayer film at the air–water interface by ozone removes the oleic acid but an organic film remains at the interface as the oleic acid is replaced by a reaction product consistent with nonanoic acid.

(b) The chemical lifetime of oleic acid at the air–water interface calculated using the results of this work is in keeping with atmospheric measurements of aged aerosol particles.

(c) Oxidation of oleic acid films on an aqueous aerosol will lower the critical supersaturation required for droplet formation.

Acknowledgements

This work was supported by SFTC ISIS grant RB15048, RB610188 and in part by NERC (NER/B/S/2003/00289). ARR is grateful to the Swedish Research Council for a travel grant.

References

1 S. D. Solomon, M. Qi, Z. Manning, M. Chen, K. B. Margquis, M. Averyt, M. Tignor and H. L. Miller, *Climate change 2007: The physical basis. Contribution of working group I to the fourth assessment report of the intergovernmental panel on climate change*, Cambridge University Press, Cambridge, UK and NY, 2007.
2 H. Tervahattu, J. Juhanoja, V. Vaida, A. F. Tuck, V. Niemi, K. Kupiainen, M. Kulmala and H. Vehkamäki, *J. Geophys. Res., [Atmos.]*, 2005, **110**, D06207; R. E. Peterson and B. J. Tyler, *Appl. Surf. Sci.*, 2003, **203**, 751; H. Tervahattu, K. Hartonen, V.-M. Kerminen, K. Kupiainen, P. Aarnio, K. Koskemtalo, A. F. Tuck and V. Vaida, *J. Geophys. Res., [Atmos.]*, 2002, **107**, 4053; H. Tervahattu, J. Juhanoja and K. Kupiainen, *J. Geophys. Res., [Atmos.]*, 2002, **107**, 4319; M. Mochida, Y. Kitamori, K. Kawamura, Y. Nojiri and K. Suzuki, *J. Geophys. Res., [Atmos.]*, 2002, **107**, 4325; L. M. Russell, S. F. Maria and S. C. B. Myneni, *Geophys. Res. Lett.*, 2002, **29**, 1779; R. E. Peterson and B. J. Tyler, *Atmos. Environ.*, 2002, **36**, 6041.
3 B. Ervens, G. Feingold and S. M. Kreidenweis, *J. Geophys. Res., [Atmos.]*, 2005, **110**, D18211.
4 M. D. King, K. C. Thompson and A. D. Ward, *J. Am. Chem. Soc.*, 2004, **126**, 16710.
5 D. J. Donaldson and V. Vaida, *Chem. Rev.*, 2006, **106**, 1445.
6 J. Zahardis and G. A. Petrucci, *Atmos. Chem. Phys.*, 2007, **7**, 1237.
7 L. F. Voss, M. F. Bazerbashi, C. P. Beekman, C. M. Hada and H. C. Allen, *J. Geophys. Res., [Atmos.]*, 2007, **112**, D06209.
8 E. González-Labrada, R. Schmidt and C. E. Dewolf, *Chem. Commun.*, 2006, 2471.
9 E. González-Labrada, R. Schmidt and C. E. Dewolf, *Phys. Chem. Chem. Phys.*, 2007, **9**, 5814.
10 Y. Wadia, D. J. Tobias, R. Stafford and B. J. Finlayson-Pitts, *Langmuir*, 2000, **16**, 9321.
11 J. R. Lu, R. K. Thomas and J. Penfold, *Adv. Colloid Interface Sci.*, 2000, **84**, 143.
12 V. F. Sears, *Neutron optics*, Oxford University Press, Oxford,1989.
13 F. Abelès, *Ann. Phys. (Leipzig)*, 1950, **5**, 611.
14 *CRC Handbook of Chemistry and Physics*, ed. D. R. Lide, CRC Press/Taylor and Francis, Boca Raton, FL, 88th edn, 2007–2008.
15 J. Hoigné, H. Bader, W. R. Haag and J. Staehelin, *Water Res.*, 1985, **19**, 993.
16 G. D. Smith, E. Woods, C. L. DeForest, T. Baer and R. E. Miller, *J. Phys. Chem. A*, 2002, **106**, 8085.
17 J. W. Morris, P. Davidovits, J. T. Jayne, K. L. Jimenez, Q. Shi, C. E. Kolb, D. R. Worsnop, W. S. Barney and G. Cass, *Geophys. Res. Lett.*, 2002, **29**, 1357.
18 J. W. Morris, P. Davidovits, J. T. Jayne, K. L. Jimenez, C. E. Kolb, Q. Shi, D. R. Worsnop, W. S. Barney and G. Cass, *J. Aerosol Sci.*, 2000, **31**, S1036.
19 W. Caetano, P. S. Haddad, R. Itri, D. Severino, V. C. Vieira, M. S. Baptista, A. P. Schröder and C. M. Marques, *Langmuir*, 2007, **23**, 1307.
20 J. B. Gilman, T. L. Eliasona, A. Fasta and V. Vaida, *J. Colloid Interface Sci.*, 2004, **280**, 234.
21 L. F. Voss, C. M. Hadad and H. C. Allen, *J. Phys. Chem. B*, 2006, **110**, 19487.
22 T. Moise and Y. Rudich, *J. Phys. Chem. A*, 2002, **106**, 6469; T. Thornberry and J. P. D. Abbatt, *Phys. Chem. Chem. Phys.*, 2004, **6**, 84; P. J. Ziemann, *Faraday Discuss.*, 2005, **130**, 469; R. L. Grimm, R. Hodyss and J. L. Beauchamp, *Anal. Chem.*, 2006, **78**, 3800; J. D. Hearn and G. D. Smith, *J. Phys. Chem. A*, 2004, **108**, 10019; H. M. Hung, Y. Katrib and S. T. Martin, *J. Phys. Chem. A*, 2005, **109**, 4517; B. W. LaFranchi, J. Zahardis and G. A. Petrucci, *Rapid Commun. Mass Spectrom.*, 2004, **18**, 2517.
23 J. D. Hearn, A. J. Lovett and G. D. Smith, *Phys. Chem. Chem. Phys.*, 2005, **7**, 501.
24 Y. Katrib, S. T. Martin, H. M. Hung, Y. Rudich, H. Z. Zhang, J. G. Slowik, P. Davidovits, J. T. Jayne and D. R. Worsnop, *J. Phys. Chem. A*, 2004, **108**, 6686.
25 H. M. Hung and P. Ariya, *J. Phys. Chem. A*, 2007, **111**, 620.
26 D. J. Last, J. J. Najera, R. Wamsley, G. Hilton, M. McGillen, C. J. Percival and A. B. Horn, *Phys. Chem. Chem. Phys.*, 2009, **11**, 1427.
27 J. Zahardis, B. W. LaFranchi and G. A. Petrucci, *J. Geophys. Res., [Atmos.]*, 2005, **110**, D08307.
28 J. C. Reynolds, D. J. Last, M. McGillen, A. Nijs, A. B. Horn, C. Percival, L. J. Carpenter and A. C. Lewis, *Environ. Sci. Technol.*, 2006, **40**, 6674; J. Zahardis, B. W. LaFranchi and G. A. Petrucci, *Atmos. Environ.*, 2006, **40**, 1661; T. M. McIntire, A. S. Lea, D. J. Gaspar, N. Jaitly, Y. Dubowski, Q. Q. Li and B. J. Finlayson-Pitts, *Phys. Chem. Chem. Phys.*, 2005, **7**, 3605; A. L. Gomez, J. Park, M. L. Walser, A. Lin and S. A. Nizkorodov, *J. Phys. Chem. A*, 2006, **110**, 3584.
29 Y. Dubowski, J. Vieceli, D. J. Tobias, A. Gomez, A. Lin, S. A. Nizkorodov, T. M. McIntire and B. J. Finlayson-Pitts, *J. Phys. Chem. A*, 2004, **108**, 10473.
30 V. F. McNeill, G. M. Wolfe and J. A. Thornton, *J. Phys. Chem. A*, 2007, **111**, 1073.
31 R. Tuckermann, *Atmos. Environ.*, 2007, **41**, 6265.
32 J. H. Seinfeld and S. N. Pandis, *Atmospheric Chemistry and Physics*, John Wiley and Sons Inc., New York, 2006.
33 B. T. Mmereki, D. J. Donaldson, J. B. Gilman, T. L. Eliason and V. Vaida, *Atmos. Environ.*, 2004, **38**, 6091; S. Raja and K. T. Valsaraj, *J. Air Waste Manage. Assoc.*, 2005, **55**, 1345.
34 M. D. King, K. C. Thompson, A. D. Ward, C. Pfrang and B. R. Hughes, *Faraday Discuss.*, 2008, **137**, 173.
35 T. Moise and Y. Rudich, *J. Geophys. Res., [Atmos.]*, 2000, **105**, 14667.
36 D. A. Knopf, L. M. Anthony and A. K. Bertram, *J. Phys. Chem. A*, 2005, **109**, 5579.
37 W. F. Rogge, L. M. Hildemann, M. A. Mazurek, G. R. Cass and B. R. T. Simonelt, *Environ. Sci. Technol.*, 1991, **25**, 1112.
38 G. L. Gaines, *Insoluble Monolayers at Liquid–Gas Interfaces*, John Wiley and Sons, New York, London, Sydney, 1966.
39 M. L. Shulman, M. C. Jacobson, R. J. Carlson, R. E. Synovec and R. E. Young, *Geophys. Res. Lett.*, 1996, **23**, 277.
40 S. Labourdenne, M. G. Ivanova, O. Brass, A. Cagna and R. Verger, *Colloids Surf., B*, 1996, **6**, 173.